

Trajectory Tracking for UAVs: An Interpolating Control Approach

Zdeněk Bouček, Miroslav Flídr, and Ondřej Straka

New Technologies for the Information Society Research Center & Department of Cybernetics

Faculty of Applied Sciences

University of West Bohemia

Pilsen, Czechia

Email: zboucek@kky.zcu.cz, flidr@kky.zcu.cz, straka30@kky.zcu.cz

Abstract—Building on our previous work, this paper investigates the effectiveness of interpolating control (IC) for real-time trajectory tracking. Unlike prior studies that focused on trajectory tracking itself or UAV stabilization control in simulation, we evaluate the performance of a modified extended IC (eIC) controller compared to Model Predictive Control (MPC) through both simulated and laboratory experiments with a remotely controlled UAV.

The evaluation focuses on the computational efficiency and control quality of real-time UAV trajectory tracking compared to previous IC applications. The results demonstrate that the eIC controller achieves competitive performance compared to MPC while significantly reducing computational complexity, making it a promising alternative for resource-constrained platforms.

Index Terms—Unmanned Aerial Vehicle, Drone, Trajectory Tracking, Model Predictive Control, Interpolating Control

I. INTRODUCTION

In UAV applications, it is important to ensure that the UAV will fly along the given trajectory. To solve this problem, trajectory tracking methods are used, which are usually implemented on-board in the Flight Control Unit or an additional on-board computing system. These methods are capable of closed-loop control, which guarantees the robustness of the system, taking into account the future course of a reference trajectory. In the tracking problem, the complex dynamics of a specific UAV can be considered along with its constraints given by structural and physical properties.

The most widely used method in UAV trajectory tracking is the Model Predictive Control (MPC) [1]–[3]. The MPC provides a solution to the problem on the receding horizon. By directly incorporating the prediction into the control strategy acquisition, the MPC is able to consider the future development of the reference trajectory. However, the consideration of a significant part of the future trajectory can lead to a major increase in complexity and thus to much higher computational time demands.

A computationally efficient alternative to the MPC can be seen in Interpolating Control (IC) [4], [5]. We have already successfully employed IC for UAV stabilization using explicit IC [6]. Unfortunately, the standard IC was designed only for control to the origin of the state space, i.e. stabilization.

Therefore, in the paper [7], we proposed a modification of the standard IC for control to a constant setpoint control. We have further extended this modification to include reference trajectory tracking [8]. Nonetheless, these modifications have so far been tested only in a simulation with a simple system.

This paper presents an algorithm based on IC for controlling the UAV along a given trajectory. The algorithm constructs a control strategy that effectively considers future states of the UAV. The resulting algorithm will be tested both in simulation and in the laboratory on the Crazyflie UAV¹.

II. TRAJECTORY TRACKING FOR UAVS

The UAV trajectory tracking aims to follow a trajectory reflecting the constraints with high precision. The constraints take into account the physical attributes of the UAVs and the restrictions imposed by the task, for example, a limited rotor speed, a restricted attitude, speed limits or to prevent the UAV from flying into a restricted area or altitude.

The trajectory tracking controller is generally implemented directly onboard the UAV, where a control code usually runs in a loop on the processor at a given frequency, so it is advantageous to consider the discrete model of the behavior. Considering these attributes, the trajectory tracking problem is often formulated as an Optimal Control Problem (OCP) [9] for discrete-time linear time-invariant systems with linear constraints and a quadratic criterion for evaluation of the control quality.

The optimization problem is in such cases formulated as

$$J(\mathbf{x}_0, \mathbf{u}_0^M) = (\mathbf{x}_M - \bar{\mathbf{x}}_M)^T \mathbf{Q} (\mathbf{x}_M - \bar{\mathbf{x}}_M) + \sum_{k=0}^{M-1} \left[(\mathbf{x}_k - \bar{\mathbf{x}}_k)^T \mathbf{Q} (\mathbf{x}_k - \bar{\mathbf{x}}_k) + \mathbf{u}_k^T \mathbf{R} \mathbf{u}_k \right]. \quad (1)$$

$$\text{s.t. } \mathbf{x}_{k+1} = \mathbf{A} \mathbf{x}_k + \mathbf{B} \mathbf{u}_k, \quad k = 0, 1, \dots, M, \quad (2)$$

$$\mathbf{x}_k \in \mathcal{X}, \quad \mathcal{X} = \{\mathbf{x}_k \in \mathcal{R}^n : \mathbf{F}^x \mathbf{x}_k \leq \mathbf{g}^x\}, \quad k = 0, 1, \dots, M, \quad (3)$$

$$\mathbf{u}_k \in \mathcal{U}, \quad \mathcal{U} = \{\mathbf{u}_k \in \mathcal{R}^m : \mathbf{F}^u \mathbf{u}_k \leq \mathbf{g}^u\}, \quad k = 0, 1, \dots, M, \quad (4)$$

where a long control horizon $M \gg 0$ is considered. The system is controlled along the given reference trajectory $\bar{\mathbf{x}}_0^M$, with each reference point along the trajectory denoted as $\bar{\mathbf{x}}_k$. The weighting matrices \mathbf{Q} and \mathbf{R} of the quadratic cost function

¹Crazyflie – www.bitcraze.io/products/crazyflie-2-1/

(1) are known symmetric positive semidefinite and positive definite, respectively. The quantities $\mathbf{x}_k \in \mathcal{R}^n$ and $\mathbf{u}_k \in \mathcal{R}^m$ are a state and control vector at time instant k , respectively.

The optimization constraints (2)-(4) are given by the dynamics of the UAV, the considered state space, and feasible control action. State space is constrained by linear inequality with matrix \mathbf{F}^x and vector \mathbf{g}^x ; control constraint inequality is defined using matrix \mathbf{F}^u and vector \mathbf{g}^u .

Many feasible solutions to the OCP (1)-(4) are based on the employment of the standard linear-quadratic regulator (LQR) law [9]. This control law is optimal for the OCP given only by (1)-(2). The LQRs used in this paper for setpoint control and trajectory tracking are based on the description in [9] and were presented in [7], [8].

A. Model Predictive Control

MPC [10] reduces the complexity of the constrained OCP by solving the OCP over a much shorter control horizon and employs a receding horizon policy, which means that at each time instant only the control \mathbf{u}_k , that is given as a solution to a particular OCP at the time instant k , is applied.

The MPC is the state-of-the-art method for trajectory tracking because it uses prediction to acquire a control strategy and at the same time it can take into account given conditions. The description of the MPC is similar to the OCP (1)-(4) with an adjusted criterion, which is in each time step given as

$$J(\mathbf{x}_k, \mathbf{u}_k^{k+N}, N) = (\mathbf{x}_N - \bar{\mathbf{x}}_N)^\top \mathbf{Q} (\mathbf{x}_N - \bar{\mathbf{x}}_N) + \sum_{l=k}^{k+N-1} [(\mathbf{x}_l - \bar{\mathbf{x}}_l)^\top \mathbf{Q} (\mathbf{x}_l - \bar{\mathbf{x}}_l) + \mathbf{u}_l^\top \mathbf{R} \mathbf{u}_l], \quad (5)$$

where N is the length of the receding horizon. The constraints (2)-(4) are the same as for OCP.

The solution to the MPC can be obtained by transcribing the problem to quadratic programming (QP) [10] which can be solved by a QP solver. The main drawback of MPC is that the solution may not be feasible or may be difficult to obtain.

B. Interpolating Control Based Trajectory Tracking

IC [4], [5] is a promising methodology applicable to the OCP. The major advantage of IC is the possibility of obtaining the control action by solving a very simple linear program (LP). This section describes IC in terms of the IC-based trajectory tracking proposed in [8].

The IC is based on the interpolation between multiple state-feedback gain control laws designed without considering inherent constraints. Using the invariant set theory [4], IC ensured the constraints were not violated.

Initial studies revealed unsatisfactory performance for standard IC-based UAV trajectory tracking. To address this, we developed a novel design of eIC that combines setpoint control and trajectory tracking LQRs. This eIC includes an additional set with a setpoint controller, while the remaining controllers are reflecting the trajectory.

1) *Invariant Sets*: The positively invariant sets used in IC design are described in [8]. We consider the system presented in Section II. Since the system (2) and the constraints (3) and (4) are considered linear, the sets are in the form of polytopes. The system is controlled by LQR.

Positively Invariant Set is defined as follows: $\Omega \subseteq \mathcal{O}$ is said to be positively invariant w.r.t. controlled system in a closed loop if and only if $\forall \mathbf{x}_k \in \Omega$. This implies that once the state $\forall \mathbf{x}_k$ reaches Ω , it will remain within Ω while satisfying the state and control constraints.

2) *State Decomposition*: The interpolation employs the principle of state decomposition, which can be denoted as

$$\mathbf{x} = c\mathbf{x}^l + (1-c)\mathbf{x}^h, \quad (6)$$

where \mathbf{x} is the state vector, c is the interpolating coefficient, $c \in \langle 0, 1 \rangle$, and \mathbf{x}^h and \mathbf{x}^l is the state vector for a high-gain and a low-gain controller, respectively. In the case of trajectory tracking, the decomposed state from Equation (6) is reflected in the IC law as

$$\mathbf{u}(\mathbf{x}_k, \bar{\mathbf{x}}_k^{k+N}) = c_k \mathbf{u}^l(\mathbf{x}_k^l, c_k \bar{\mathbf{x}}_k^{k+N}) + (1-c_k) \mathbf{u}^h(\mathbf{x}_k^h, (1-c_k) \bar{\mathbf{x}}_k^{k+N}), \quad (7)$$

where $\mathbf{u}^h(\mathbf{x}_k^h, \bar{\mathbf{x}}_k^{k+N})$ is the high-gain control law for \mathbf{x}_k^h and $\mathbf{u}^l(\mathbf{x}_k^l, \bar{\mathbf{x}}_k^{k+N})$ is the low-gain control law for \mathbf{x}_k^l . The setpoint control law is obtained by substituting $\bar{\mathbf{x}}_k^{k+N}$ with $\bar{\mathbf{x}}_k$.

While both controllers could be used by simply switching between them based on the system's current state, it would introduce discontinuity in the control. Moreover, in the region $\Omega^l \setminus \Omega^h$, it would lead to slower convergence of the system state towards the desired region of the state space.

3) *Interpolating Control*: As has been said, the standard IC depends on finding the optimal interpolation coefficient c^* , which can be acquired by minimizing the criterion in simple LP, which was described for setpoint control in [7] and for trajectory tracking in [8]. The LP adjusts to setpoint control or trajectory tracking by shifting the center of set Ω^h of the high-gain controller $\mathbf{u}^h(\mathbf{x}_k^h, \bar{\mathbf{x}}_k^{k+N})$ from the origin coordinates to the setpoint or current point of reference trajectory coordinates.

4) *Extended Interpolating Control*: In case the set $\Omega^l \setminus \Omega^h$ is large, the performance of the IC can be degraded. The performance can be usually improved by adding an intermediate invariant set $\Omega^l \subset \Omega^m \subset \Omega^h$, where another intermediate state-feedback controller is defined. This extended version of IC is called eIC for clarity. In case \mathbf{u}^h is LQR, \mathbf{u}^m can be obtained for example with an increase in the weight \mathbf{R} . The set Ω^m is calculated as Ω^h .

The eIC modification for trajectory tracking presents challenges, as discussed in [8]. To ensure that $\bar{\mathbf{x}}_k^{k+N} \in \Omega^m$ when controlling within the region $\Omega^m \setminus \Omega^h$, adjustments must be made to the reference trajectory. These adjustments become even more complex because the center of set Ω^m is also shifted to the coordinates of the current reference trajectory point.

In eIC, there are two distinct LPs. If $\mathbf{x} \in \Omega^l \setminus \Omega^m$, the interpolation is done between \mathbf{u}^l and \mathbf{u}^m and the IC control law takes the form of

$$\mathbf{u}(\mathbf{x}_k, \bar{\mathbf{x}}_k^N) = c_k \mathbf{u}^l(\mathbf{x}_k^l, c_k \bar{\mathbf{x}}_k^N) + (1-c) \mathbf{u}^m(\mathbf{x}^m, (1-c_k) \bar{\mathbf{x}}_k). \quad (8)$$

If the $\mathbf{x} \in \Omega^m$, the interpolation is performed for both \mathbf{u}^m and \mathbf{u}^h , which results in control law

$$\mathbf{u}(\mathbf{x}_k, \bar{\mathbf{x}}_k^N) = c_k \mathbf{u}^m(\mathbf{x}_k^m, c_k \bar{\mathbf{x}}_k) + (1 - c_k) \mathbf{u}^h(\mathbf{x}_k^h, (1 - c_k) \bar{\mathbf{x}}_k^N). \quad (9)$$

III. PLANAR UAV MODEL AND CONTROL DESIGN

Both MPC and IC are model-based methods. Their design requires knowledge of the behavior model of the controlled system. Therefore, this section outlines the behavioral model of UAVs. Additionally, it outlines constraints based on the UAV's characteristics and flight space. Finally, it describes the parameters of each UAV controller.

A. Planar UAV Model

For easier analysis and better insight, a planar UAV model (see Figure 1) will be employed, which exhibits similar behavior but is reduced both in the number of state variables and in the complexity of the equations of motion. The dynamics along \bar{y} and \bar{z} -axis with attitude ϕ as rotation around axis \bar{x} are considered.

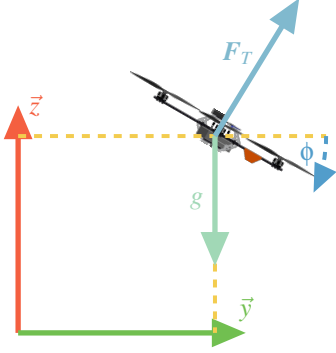


Fig. 1: Planar UAV in the local frame

The nonlinear dynamics of the planar UAV is described by the following equations

$$\ddot{y}(t) = -\frac{F_T(t)}{m} \sin(\phi(t)), \quad \ddot{z}(t) = -g + \frac{F_T}{m} \cos(\phi(t)), \quad \ddot{\phi}(t) = \frac{\tau_{R_x}(t)}{J_x}, \quad (10)$$

where F_T is the collective thrust in [N], m is the mass of the UAV in [kg], τ_{R_x} is the collective torque in [N · m] generated by rotors around \bar{x} -axis and J_x is the moment of inertia around \bar{x} in [kg · m²].

The attitude control is handled by the UAV's autopilot, the proposed controller can control the translation in \bar{y} and \bar{z} via desired acceleration, which is recalculated based on linearized equations (10) around hover state to attitude control reference as

$$\bar{\phi}(t) = -\frac{\ddot{y}(t)}{g}, \quad F_T(t) = m(\ddot{z}(t) + g), \quad (11)$$

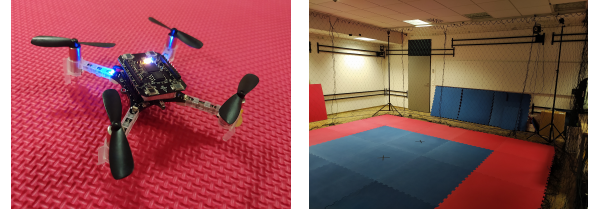
where $\bar{\phi}$ and F_T are desired angle and collective thrust, respectively. Moreover, as a side effect, the controllers are independent of the UAV's parameters m and J_x , as they are only compensated in the calculations for the attitude and thrust control setpoint.

B. Model Parameters

The model parameters were selected to align with a real UAV, specifically, the Crazyflie 2.0 developed by Bitcraze (see Figure 2a). Similarly, the state and control constraints were set using both experimentally measured and manufacturer-provided values. Regarding the model's parameters, we set the UAV's mass to $m = 0.03$ kg and the moment of inertia to $J_x = 2.3951 \cdot 10^{-5}$ kg · m². State and control constraints were defined as

$$\begin{aligned} -2 \leq y \leq 2, \quad -1.25 \leq z \leq 1.25, \quad [\text{m}], \\ -5 \leq \dot{y} \leq 5, \quad -5 \leq \dot{z} \leq 5, \quad [\text{m/s}], \end{aligned}$$

where the position constraints align with the laboratory parameters (see Figure 2b), and the velocity constraints are set to allow high-performance maneuvers. The lower bound for the position in the \bar{z} -axis is negative to enable stabilization control, while \bar{z} is transformed to have system origin at a height of 1.25 m.



(a) Crazyflie UAV

(b) Flight arena

Fig. 2: Laboratory Experiment with Crazyflie UAV

C. Controllers Design

The weights of the quadratic criterion used in designing the controllers were appropriately selected based on the UAV's behavior and surrounding environment as

$$\begin{aligned} \mathbf{Q}_y^h = \begin{bmatrix} 0.16 & 0 \\ 0 & 0.04 \end{bmatrix}, \quad \mathbf{Q}_z^h = \begin{bmatrix} 0.64 & 0 \\ 0 & 0.04 \end{bmatrix}, \\ \mathbf{R}_y^h = \frac{1}{2} \cdot 0.15 \cdot \frac{4}{0.03} \cdot \sin 30^\circ = 5, \quad \mathbf{R}_z^h = 5^{-2} = 0.04, \end{aligned}$$

where \mathbf{Q}_y^h , \mathbf{R}_y^h , \mathbf{Q}_z^h , and \mathbf{R}_z^h are the weights utilized in MPC, IC, and eIC for position control in \bar{y} and \bar{z} -axis.

For trajectory tracking, IC employs the LQR \mathbf{u}^l with the following weight configuration:

$$\begin{aligned} \mathbf{Q}_y^l = \begin{bmatrix} 0.25 & 0 \\ 0 & 0.04 \end{bmatrix}, \quad \mathbf{Q}_z^l = \begin{bmatrix} 0.64 & 0 \\ 0 & 0.04 \end{bmatrix}, \\ \mathbf{R}_y^l = 10 \cdot \mathbf{R}_y^h = 50, \quad \mathbf{R}_z^l = 10 \cdot \mathbf{R}_z^h = 0.4. \end{aligned}$$

The setpoint LQR \mathbf{u}^m uses the following weighting matrices

$$\mathbf{Q}_y^m = \mathbf{Q}_y^l, \quad \mathbf{Q}_z^m = \mathbf{Q}_z^l, \quad \mathbf{R}_y^m = \mathbf{R}_y^h, \quad \mathbf{R}_z^m = \mathbf{R}_z^h. \quad (12)$$

The predictive horizon was set to 8s as in [1], resulting in $N = 800$ steps for the $T_s = 0.01$ s discrete model. However, such a long horizon is not feasible for real-time MPC implementation. To address the issue, we employed the move blocking technique [11], which fixes the control variable values \mathbf{u}_k^{k+N} for multiple time steps, reducing the QP's degrees of freedom. To further reduce complexity, the prediction for $T_s = 0.01$ s is performed

only in the first step and afterward, the model with $T_s = 0.2s$ is considered. The complexity of the problem was reduced by 95%. This version of the MPC will be referred to hereafter as MPCMB.

A basic discrete-time PID controller is implemented in Python with experimentally obtained parameters $K_p = 0.3$, $K_d = 0.003$, and $K_i = 0.0001$, and with a period $T_{s_att} = 0.001s$. The PID simulates the attitude control behavior in a scenario with the planar UAV model, which would otherwise be done by the autopilot.

IV. EXPERIMENTAL SETUP

The experiments are conducted using both a planar model simulation and a 3D simulation environment Gym-PyBullet-Drones [12], and with the Crazyflie UAV wirelessly controlled in the laboratory utilizing the cflib library². The MPC has been excluded from real-world and Gym-Pybullet-Drones tests due to its high computational complexity.

Simulations are executed on a desktop PC with an Intel Core i9-9900 and 64GB DDR4 RAM, running Ubuntu 22 and Python 3.8. The LPs and QPs were modeled using CVXPY and solved using GUROBI [13]. In the laboratory experiment, a laptop with Intel Core i7-8550 and 16GB DDR3 RAM is used with the same software setup.

Tracking was performed for two types of reference trajectories: the Ellipse and the Lemniscate of Gerono. As both trajectories delivered similar results, only the Lemniscate is presented.

A. Simulations

The planar model is implemented in Python based on the non-linear dynamics described in (10). The reference signal for lemniscate was generated for \vec{x} and \vec{y} axes. Other reference states are equal to zero vectors, however, since the reference signal is time-parameterized, it is, therefore, the trajectory.

The response is tested for angular frequencies $\omega_s = 0.4$ and $\omega_s = 0.6$. For $\omega_s = 0.6$, the reference is referred to as a high-frequency lemniscate trajectory. The simulation begins with the initial condition at the state space origin, with a nonzero reference requiring initial convergence.

The Gym-PyBullet-Drones [12] is a simulation environment for single and multi-agent reinforcement learning with nano quadcopters. To test controllers under more practical circumstances, this environment features the simulation of Crazyflie UAV. The lemniscate trajectory is set in the \vec{x} and \vec{y} axes, while the \vec{z} -axis is set to a faster-oscillating signal to provide a more complex test of the \vec{z} -controller.

Since this is a 3D simulation, the \vec{y} -axis controller is also used for controlling the \vec{x} -axis. The output of the \vec{x} and \vec{y} controllers must be rotated around the \vec{z} -axis in order reflect the UAV's yaw angle ψ .

B. Laboratory Experiment with Crazyflie UAV

The laboratory experiments use Crazyflie 2.0 UAVs equipped with the Lighthouse positioning deck³, which enables UAV's self-localization via the HTC SteamVR Base Station 2.0 with high accuracy.

MPCMB exhibits excessively long computation times during experiments, exceeding the expected $T_s = 0.01s$. The UAV is unable to stabilize in the \vec{z} -axis and keeps oscillating, resulting in a crash. To address this issue, two types of experiments are conducted: First, MPCMB generates roll and pitch angle and the \vec{z} position is directly set using `send_zdistance_setpoint` function. Secondly, the thrust is controlled by ICs using the function `send_setpoint`. For ICs, parallel computing is also tested using Pool from the multiprocessing library. The trajectory was adjusted for safety purposes and was slightly smaller.

V. RESULTS AND DISCUSSION

The controllers are evaluated for tracking a lemniscate reference trajectory in terms of control quality and computational complexity. Control quality is assessed based on the quadratic criterion, the integral square error (ISE), and the energy required to control the UAV.

The quadratic criterion value in Equation (1) is weighted by the inverse of T_s . In contrast, the ISE evaluates the accuracy of the reference position tracking. For example, for position x the ISE is calculated as

$$ISE = \frac{1}{T_s} \sum_{k=0}^n e_k^2, \quad (13)$$

where $e_k = (\bar{x}_k - x_k)$. The presented ISE value is the sum of the ISE from all axes. The energy is directly dependent on the controller output, which is by design given as the desired acceleration. To illustrate, for the \vec{z} -axis controller, energy is assessed using the following equation

$$E = \frac{1}{T_s} \sum_{k=0}^n \ddot{z}_k^2. \quad (14)$$

In laboratory experiments, the criteria cannot be weighted solely by T_s due to asynchronous communication and delays resulting from the control action calculation. Thus, the difference between time instants $t_k - t_{k-1}$ is used to weight the individual elements. The evaluation of controller time demands is based on total, average, and maximum computation time. For laboratory experiments, the number of calculated control actions is also included.

A. Simulations

When $\omega_s = 0.4$ s, the controllers exhibit similar behavior. The difference is observed only at the beginning, where ICs and MPCs have quite different paths. The interpolating coefficients are zero except at the very beginning of the simulation in the \vec{y} -axis. Thus, the ICs achieved optimal behavior for the most of time. In Table I, we can see the interpolation-based controllers

²CFLib – <https://github.com/bitcraze/crazyflie-lib-python>

³LH deck – www.bitcraze.io/lighthouse-positioning-deck

TABLE I: Evaluation of control quality with the planar UAV model (2D) and Gym-PyBullet-Drones (3D) simulation

2D $\omega_s = 0.4$	J	%	ISE	%	E	%
MPC	7.07	-	1.76	-	21.20	-
MPCMB	7.74	+9.48	2.19	+24.43	16.80	-20.75
eIC	8.23	+16.41	1.73	-1.70	27.30	+28.77
IC	8.68	+22.77	1.50	-14.77	33.80	+59.43
2D $\omega_s = 0.6$	J	%	ISE	%	E	%
MPC	13.60	-	2.02	-	61.20	-
MPCMB	15.70	+15.44	2.64	+30.69	58.30	-4.74
eIC	16.40	+20.59	1.73	-14.36	79.30	+29.58
IC	23.50	+72.79	3.86	+91.09	98.00	+60.13
3D $\omega_s = 0.6$	J	%	ISE	%	E	%
MPCMB	52.8	-	6.40	-	2.79	-
eIC	73.8	+39.77	2.71	-57.66	3.77	+35.13
IC	192	+263.64	5.20	-18.75	4.68	+67.74

are worse in optimality criterion because they consumed more energy. However, they followed the trajectory more closely.

Very different results were obtained for the high-frequency trajectory with $\omega_s = 0.6$ s. According to Figure 3, the ICs again tried to follow the reference faster. The IC deviates significantly at two points, possibly due to the interaction between controllers, which may cause this issue. As the \bar{y}^L controller increases the ϕ angle for greater acceleration, it can lead to a deflection of the thrust controlled by the \bar{z}^L controller. According to the optimality criterion, Table I demonstrates that the MPC produced the most favorable outcomes. However, the eIC again followed the trajectory closest. In contrast, the IC achieved the worst results by all criteria.

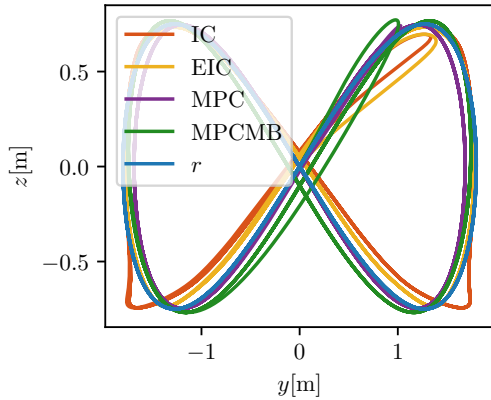


Fig. 3: Path from tracking the high-frequency trajectory with the planar model

In the 3D simulation environment, the results for $\omega_s = 0.4$ are comparable to those of the planar model, only the case of the high-frequency lemniscate will be presented. The MPCMB achieved the best optimality criterion value, as seen in Table I. The IC was too aggressive, consuming excessive energy, and its optimality criterion value was 264% higher than the MPCMB. In contrast, the eIC performed 40% worse than the MPCMB in terms of the optimality criterion but had precise trajectory tracking. The eIC attained substantially lower ISE than the MPCMB while maintaining reasonable energy use.

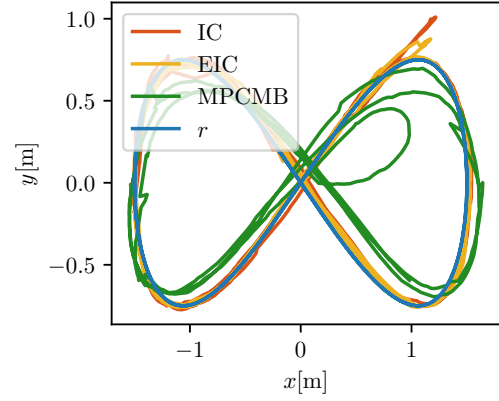


Fig. 4: Path from tracking the high-frequency trajectory with Crazyflie UAV in laboratory

TABLE II: The control quality in the laboratory experiment

2D	J	%	ISE	%	E	%
MPCMB	9.67	-	3.85	-	0.42	-
eIC	10.70	+10.65	1.42	-63.12	1.09	+161.39
IC	11.10	+14.79	1.39	-63.90	1.17	+180.58
3D	J	%	ISE	%	E	%
eIC par	20.2	-	1.56	-	1.62	-
IC par	21.1	+4.46	1.61	+3.21	1.65	+1.85
eIC	19.9	-1.49	1.57	+0.64	1.68	+3.70
IC	24.7	+22.28	1.73	+10.90	2.09	+29.01

B. Laboratory Experiments with Crazyflie UAV

Since the controllers only handle Crazyflie's motion in the \bar{x}^L and \bar{y}^L axes, the presented plots show the controllers' performance exclusively in those axes. During lab testing, the ICs promptly followed the reference (Figure 4). In contrast, the MPCMB maneuvered the path at a slower pace, resulting in a smaller path. The MPCMB attained the lowest cost, while the ICs had 10–15% higher values (Table II). Nevertheless, both ICs tracked the trajectory more accurately based on the ISE, but at significantly higher energy consumption.

For the 3D control, the captured UAV path is very similar for all ICs (Figure 5). There are minor differences between the standard and parallelized versions of the controllers. Furthermore, we can see a significant change in one point in case of standard eIC. Such a sudden change can be explained by a poor estimate of the UAV's position. However, all ICs successfully track the reference trajectory.

The performance evaluation shown in Table II indicates that both eICs yield comparable results. That said, the standard eIC outperforms the parallel eIC in terms of the optimality criterion, despite consuming more energy and deviating slightly according to ISE. The values of the weighting matrices and the small differences in the behavior of both controllers cause this paradox. Interestingly, the parallel IC is only 4.5% worse than the parallel eIC, which is even more intriguing since the standard IC is 22.3% worse.

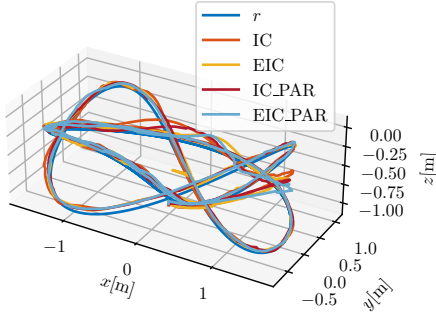


Fig. 5: Path from 3D tracking the high-frequency trajectory with Crazyflie UAV in laboratory

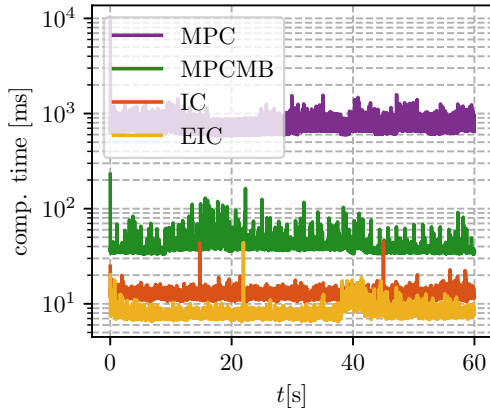


Fig. 6: Computational time for tracking the fast lemniscate trajectory with a planar model of the UAV

C. Computational Demands

The computational demands are consistent for all scenarios. Therefore, only the results for the high-frequency lemniscate trajectory are presented.

The logarithmic plot in Figure 6 indicates the MPC took the longest computation time, followed by MPCMB. IC and eIC have comparable demands with eIC faster the most of time, likely due to the shape of the Ω^m set and LP. Table III confirms the order of magnitude differences, also for 3D simulation. The findings demonstrate that IC is a highly time-efficient substitute for MPC. For MPCs, it is evident that the initial computational time is significantly longer than subsequent times. This may be due to the solver utilizing the previous step's results in the following step.

In the lab tests, a noticeable difference is observed between the ICs (see Table IV). It is important to note that the previous tests were conducted on a desktop computer, while the lab test was conducted on a laptop. Parallelized IC demonstrates lower maximum times, whereas parallel eIC has slightly higher averages. Nonetheless, parallel IC exhibited improved performance over standard IC based on all metrics. Overall, the standard eIC remained the most efficient.

TABLE III: The time demands with the planar UAV model (2D) and Gym-PyBullet-Drones (3D) simulation

	2D	t [s]	%	t_{\max} [ms]	%
MPC		4180	-	9507	-
MPCMB		247	-94.09	230	-97.58
eIC		49	-98.83	44	-99.54
IC		75	-98.21	45	-99.53
	3D	t [s]	%	t_{\max} [ms]	%
MPCMB		335	-	374	-
eIC		72	-78.51	68	-81.82
IC		109	-67.46	51	-86.36

TABLE IV: The time demands in the laboratory experiment

	2D	t [s]	%	N_s	%	\bar{t} [ms]	%	t_{\max} [ms]	%
MPCMB		30	-	582	-	51	-	432	-
eIC		26	-13.33	2658	+356.70	10	-80.39	118	-72.69
IC		30	+0.00	1407	+141.75	21	-58.82	120	-72.22
	3D	t [s]	%	N_s	%	\bar{t} [ms]	%	t_{\max} [ms]	%
eIC par		29	-	1648	-	18	-	73	-
IC par		30	+3.45	1153	-30.04	26	+44.44	67	-8.22
eIC		30	+3.45	2106	+27.79	14	-22.22	106	+45.21
IC		30	+3.45	993	-39.75	30	+66.67	125	+71.23

VI. CONCLUSION AND FUTURE WORK

The UAV trajectory tracking controllers underwent both simulated and laboratory testing. The evaluation compared controller performance in both control quality and computational complexity. Generally, MPCs showed superior performance, especially in terms of optimality. Even so, ICs can provide comparable performance and serve as a viable alternative to MPCs due to their computational efficiency, especially on devices with limited computing power.

Our research suggests that the eIC is a promising controller for trajectory tracking, displaying faster computation times and enhanced accuracy in comparison to IC. Additionally, parallel versions of ICs have shown further reductions in computation time. Integrating the IC directly into the autopilot of the Crazyflie UAV in the future could potentially advance trajectory tracking. Although, careful consideration of the platform's limitations would be necessary.

REFERENCES

- [1] T. Baca, P. Stepan, V. Spurny, D. Hert, R. Penicka, M. Saska, J. Thomas, G. Loianno, and V. Kumar, "Autonomous landing on a moving vehicle with an unmanned aerial vehicle," *Journal of Field Robotics*, vol. 36, no. 5, pp. 874–891, 2019. [Online]. Available: <https://onlinelibrary.wiley.com/doi/abs/10.1002/rob.21858>
- [2] M. Kamel, M. Burri, and R. Siegwart, "Linear vs Nonlinear MPC for Trajectory Tracking Applied to Rotary Wing Micro Aerial Vehicles," *IFAC-PapersOnLine*, vol. 50, no. 1, pp. 3463–3469, 2017.
- [3] T. Nascimento and M. Saska, "Embedded Fast Nonlinear Model Predictive Control for Micro Aerial Vehicles," *Journal of Intelligent & Robotic Systems*, vol. 103, no. 4, p. 74, dec 2021. [Online]. Available: <https://link.springer.com/10.1007/s10846-021-01522-y>
- [4] H. Nguyen, *Constrained Control of Uncertain, Time-Varying, Discrete-Time Systems: An Interpolation-Based Approach*, ser. Lecture Notes in Control and Information Sciences. Springer International Publishing, 2014.
- [5] S. Scialanga and K. Ampountolas, "Interpolating Control Toolbox (ICT)," in *2019 18th European Control Conference (ECC)*. IEEE, jun 2019, pp. 2510–2515. [Online]. Available: <https://ieeexplore.ieee.org/document/8796000/>
- [6] Z. Bouček and M. Flidr, "Explicit Interpolating Control of Unmanned Aerial Vehicle," in *Proc. of the 24th International Conference on Methods and Models in Automation and Robotics*, Miedzyzdroje, Poland, August 26–29 2019.

- [7] —, “Modification of Explicit Interpolating Controller for Control Problem with Constant Setpoint,” in *Proc. of the 15th European Workshop on Advanced Control and Diagnosis, ACD 2019*, Bologna, Italy, November 21–22 2019.
- [8] —, “Interpolating Control Based Trajectory Tracking *,” in *2020 16th International Conference on Control, Automation, Robotics and Vision (ICARCV)*. IEEE, dec 2020, pp. 701–706. [Online]. Available: <https://ieeexplore.ieee.org/document/9305511/>
- [9] B. Anderson and J. Moore, *Optimal Control: Linear Quadratic Methods*, ser. Dover Books on Engineering. Dover Publications, 2007.
- [10] F. Borrelli, A. Bemporad, and M. Morari, *Predictive Control for Linear and Hybrid Systems*. Cambridge University Press, 2017.
- [11] R. Cagienard, P. Grieder, E. Kerrigan, and M. Morari, “Move blocking strategies in receding horizon control,” *Journal of Process Control*, vol. 17, no. 6, pp. 563–570, jul 2007. [Online]. Available: <https://linkinghub.elsevier.com/retrieve/pii/S0959152407000030>
- [12] J. Panerati, H. Zheng, S. Zhou, J. Xu, A. Prorok, and A. P. Schoellig, “Learning to fly—a gym environment with pybullet physics for reinforcement learning of multi-agent quadcopter control,” in *2021 IEEE/RSJ International Conference on Intelligent Robots and Systems (IROS)*, 2021.
- [13] Gurobi Optimization, LLC, “Gurobi Optimizer Reference Manual,” 2023. [Online]. Available: <https://www.gurobi.com>